Electronic Supplementary Material (ESI) for Journal of Materials Chemistry C.

Supporting Information

Porphyrin based metal-organic frameworks: highly sensitive materials for optical sensing of oxygen in gas phase

Tobias Burger,[1] Christian Winkler,[2] Irene Dalfen,[1] Christian Slugovc,[3*]
Sergey M. Borisov[1*]

[1] *Graz University of Technology, Institute of Analytical Chemistry and Food Chemistry; Stremayrgasse 9; 8010 Graz; Austria*

[2] *Graz University of Technology, Institute of Solid State Physics; Petersgasse 16; 8010 Graz; Austria*

[3] *Graz University of Technology, Institute of Institute for Chemistry and Technology of Materials; Stremayrgasse 9; 8010 Graz; Austria*

Chemicals and materials

5,10,15,20-Tetrakis-(4-carboxyphenyl)-21,23H-porphyrin was obtained from Porphyrin laboratories (www.porphyrin-laboratories.com, Gleschendorf, Gemany). K_2CO_3 was from Sigma Aldrich (www.sigmaaldrich.com). Methyl iodide was obtained from Acros (www.acros.com). Ethylacetate, tetrahydrofuran (THF), NaOH, cyclohexane, HCl, toluene, benzonitrile and methanol were from VWR (www.vwr.com). $TaCl_5$, $PdCl_2$ and $PtCl_2$ were obtained from ABCR (www.abcr.com). (1-Trimethylsilyl)-1-propyne (TMSP) was from TCI chemicals (www.tcichemicals.com). Silica gel 60 H and diethyl ether were from Merck. N, N-dimethylformamide (DMF) was from Roth (www.carlroth.com). Deuterated chloroform ($CDCl_3$) and deuterated dimethyl sulfoxide-d_6 (DMSO-d_6) were from Eurisotop.

The synthesis of Pd(II)TCPP was done in a Monowave 50 synthesis reactor from Anton Paar (www.anton-paar.com, Graz, Austria).

cis-Bis((benzonitrile)dichloroplatinum(II) was prepared by refluxing $PtCl_2$ in benzonitrile for 1 h and precipitating the resulted product in cyclohexane.

Synthesis of 5,10,15,20-tetrakis-(4-carboxyphenyl)-porphyrin-Pt(II) (Pt(II)TCPP)

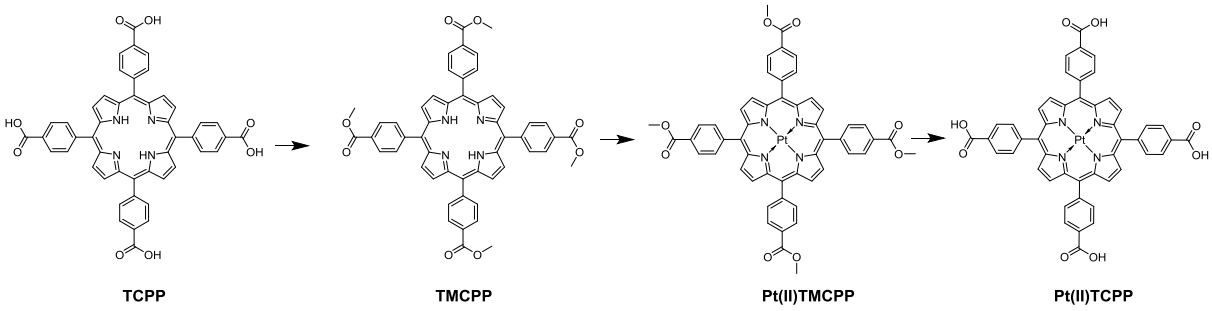

Scheme S1. Synthesis of Pt(II)TCPP

Pt(II)TCPP was synthesized via 5,10,15,20-tetrakis(4-methoxycarbonyl)phenyl)porphyrin (H_2TMCPP) according to a literature method.[1] In short, 300 mg (373 µmol) 5,10,15,20-tetrakis-(4-carboxyphenyl)-21,23H- porphyrin were dissolved in 90 mL DMF and 402 mg (2.91 mmol) K_2CO_3 were added. After addition of 1.08 g (7.61 mmol) methyl iodide the reaction was stirred for 24 h at 140 °C. After cooling to room temperature, the crude reaction mixture was poured into water and the product extracted with ethyl acetate and washed with water. After chromatographic purification on silica gel using ethyl acetate as an eluent, TMCPP was obtained as a purple, crystalline solid. 260 mg product (yield 80%) were obtained.

Metalation and deprotection of the methyl esters was done by a modified procedure:[2]

70 mg (83 µmol) of H_2TMCPP were dissolved in 50 ml benzonitrile in a Schlenk flask. Oxygen was removed by bubbling argon through the solution while vigorously stirring. 78 mg (165 µmol) cis-bis((benzonitrile)dichloroplatinum(II) were added and the solution was heated at 150 °C overnight. After the reaction was completed as indicated by UV-VIS spectroscopy, the solution was cooled to room temperature. The product was precipitated in 200 mL cyclohexane. The crude product was filtered through silica gel and washed thoroughly with cyclohexane. The product was eluted from the silica gel bed with THF. 100 mg crude product were obtained and directly used without any further purification in the next step.

100 mg crude Pt(II)TMCPP were dissolved in 50 mL THF and 3 mL 1M aq. NaOH were added. The solution was stirred at 65 °C overnight and cooled to room temperature. After reaction completion indicated by TLC, the product was precipitated by dropwise addition of 1M HCl. The precipitate was separated by centrifugation and washed 2x with water. After drying at 65 °C in vacuum, platinum(II) 5,10,15,20-tetrakis-(4-carboxyphenyl)-porphyrin (Pt(II)TCPP) was obtained as a red powder (60 mg, 73%).

TMCPP: ^{1}H NMR (300MHz, $CDCl_3$): δ (ppm) 8.82(s, 8H), 8.45 (d, J = 8.0 Hz, 8H), 8.29 (d, J = 8.0 Hz, 8H), 4.11(s, 12H), -2.8 (s, 2H)

Pt(II)TMCPP: ^{1}H NMR (300 MHz, $CDCl_3$) δ (ppm) 8.72 (s, 8H), 8.43 (d, J = 7.9 Hz, 8H), 8.23 (d, J = 8.0 Hz, 8H), 4.10 (s, 12H).

Pt(II)TCPP: ^{1}H NMR (300 MHz, DMSO-d_6) δ (ppm) 13.31 (s, 4H), 8.76 (s, 8H), 8.37 (d, J = 8.0 Hz, 8H), 8.29 (d, J = 8.0 Hz, 8H).

Synthesis of 5,10,15,20-Tetrakis-(4-carboxyphenyl)-porphyrin-Pd(II) (Pd(II)TCPP)

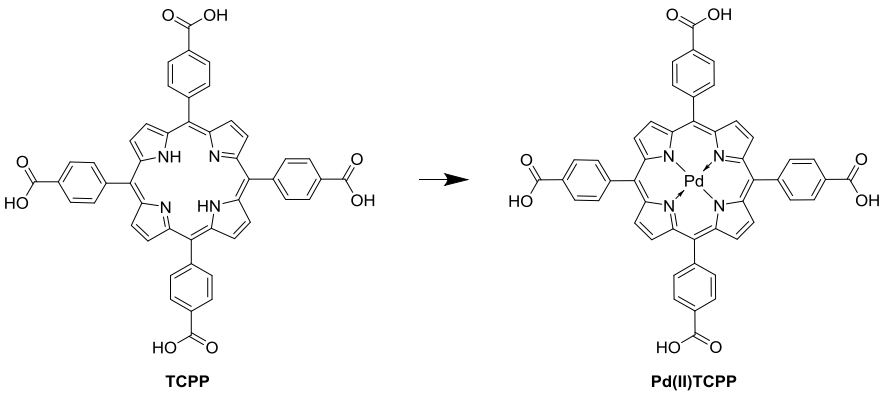

Scheme S2. Synthesis of Pd(II)TCPP.

Pd(II)TCPP was synthesized according to a reported procedure.[3] 65 mg (82 µmol) of 5,10,15,20-tetrakis-(4-carboxyphenyl)-21,23H-porphyrin were dissolved in 4 mL DMF in a 10 mL microwave-suitable borosilicate vial. 60 mg (338 µmol) of palladium dichloride was added, the reaction vessel was closed and heated in a synthesis reactor at 155 °C for 15 minutes. Completion of the reaction was controlled after cooling to room temperature by UV-VIS spectroscopy. The resulting solution was filtered to remove colloidal palladium, diluted with THF : diethyl ether (2:1 v/v), filtered and washed with 3 x 20 mL water. All solvents were removed and the product was dried at 65 °C in vacuum. 55 mg product (74.8%) were obtained as a red powder.

^{1}H NMR (300 MHz, DMSO) δ 8.82 (s, 8H), 8.37 (d, J = 8.2 Hz, 8H), 8.30 (d, J = 8.1 Hz, 8H).

Synthesis of poly(trimethylsilylpropyne) (PTMSP)

Polymerization of TMSP was carried out in a dry box as follows.[4] $TaCl_5$ (0.5 g, 1.4 mmol) was dissolved in 0.1 L of toluene. The mixture was stirred for 30 min at room temperature. 12 g (107 mmol) of TMSP were added to this catalyst solution. The mixture immediately turned dark brown and the solution solidified within 30 min. After 24 h the polymerization mixture was worked up by precipitation of the polymer in rapidly stirred 200 mL hot methanol. The polymer was washed several times with hot methanol and then dried to a constant weight. A yield of 95% (11.4 g) was achieved.

Analysis of the PXRD Measurements of MOF PCN-224 and Pt(II)PCN-224

Powder x-ray diffraction (PXRD) measurements were performed at the XRD1 beamline at the Elettra Synchrotron in Triest. This beamline has an operating wavelength of 1.4 Å with a beam size of 200 x 200 µm^2. The data was collected on a stationary Dectris Pilatus 2M detector which was mounted 400 mm away from the sample. The sample itself consisted of the lab-synthesized MOF PCN-224 powder which was filled in a glass capillary (1.5 mm diameter and 0.02 mm wall thickness). All data were transformed to reciprocal space for analysis. All data conversion, treatment and analysis steps were performed with GIDVis.[5] Two samples were prepared and characterized: (i) Pt(II)PCN-224 and (ii) PCN-224.

Pt(II)PCN-224

The measured data for this system were compared to known structures for two PCN-224 based MOFs, one MOF consisting of Ni(II) metalated TCPP (Ni(II)TCPP) and the other based on the metal-free porphyrin.[6] The reported structures (see Fig. S1) are cubic and belong to space group Im-3m (no. 229). To mimic the Pt(II)PCN-224 MOF we replaced the Ni atom in the literature structure by Pt.

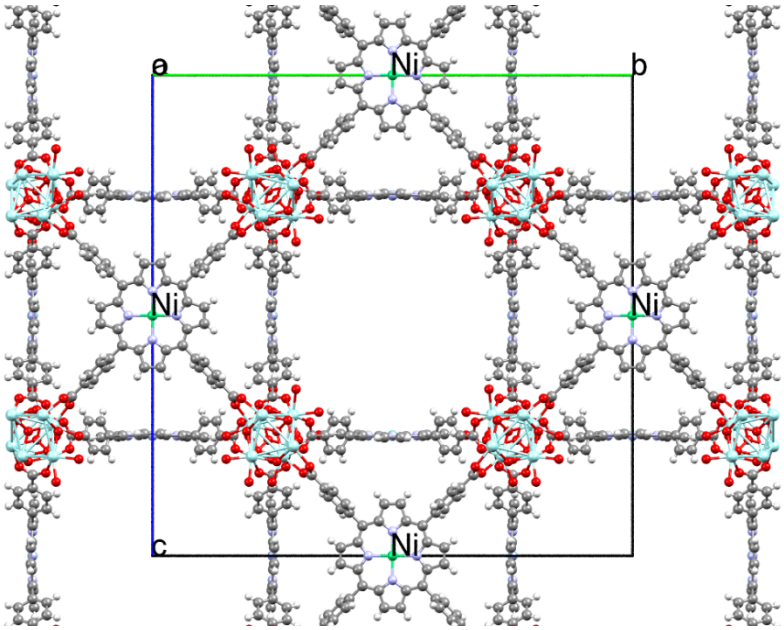

Fig. S1. Crystal structure of the Ni metalated MOF reported in Ref [6].

In Fig. S2 one can see the PXRD pattern of Pt(II)PCN-224 as measured at the synchrotron. The peak positions of PCN-224 are overlaid as dashed black lines. One can see that the peak positions agree well for these two structures. This agreement also allows the indexation of corresponding peaks. Replacing the Ni atoms by Pt atoms in our model structure one can calculate new peak positions that agree with the ones of the measured data within the experimental accuracy, as expected (see Fig. S3). Please note that the measured data presented in Fig. S2 and S3 is the same, only the model structure, the measurements are compared to, changes.

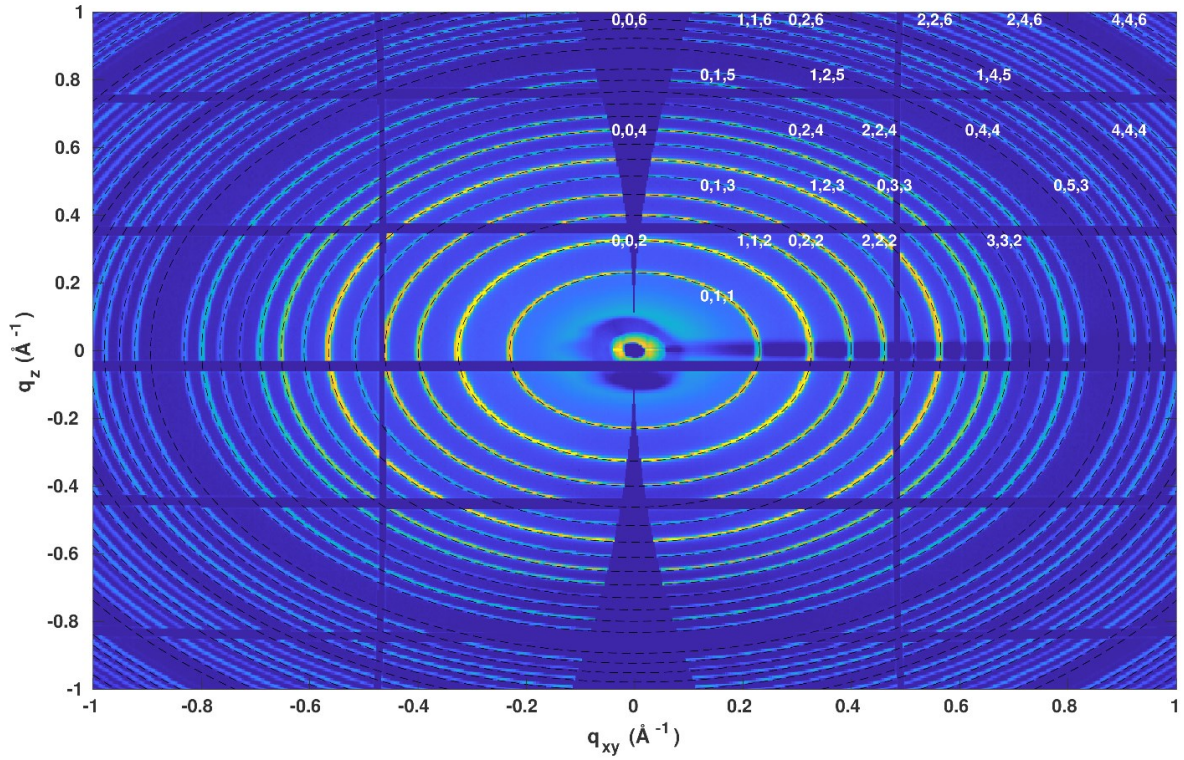

Fig. S2. Synchrotron PXRD patterns of Pt(II)PCN-224. The dashed lines are the peak positions determined by the structure of the Ni metallated PCN-224 from Ref [6]. The labels in white are the Laue indices.

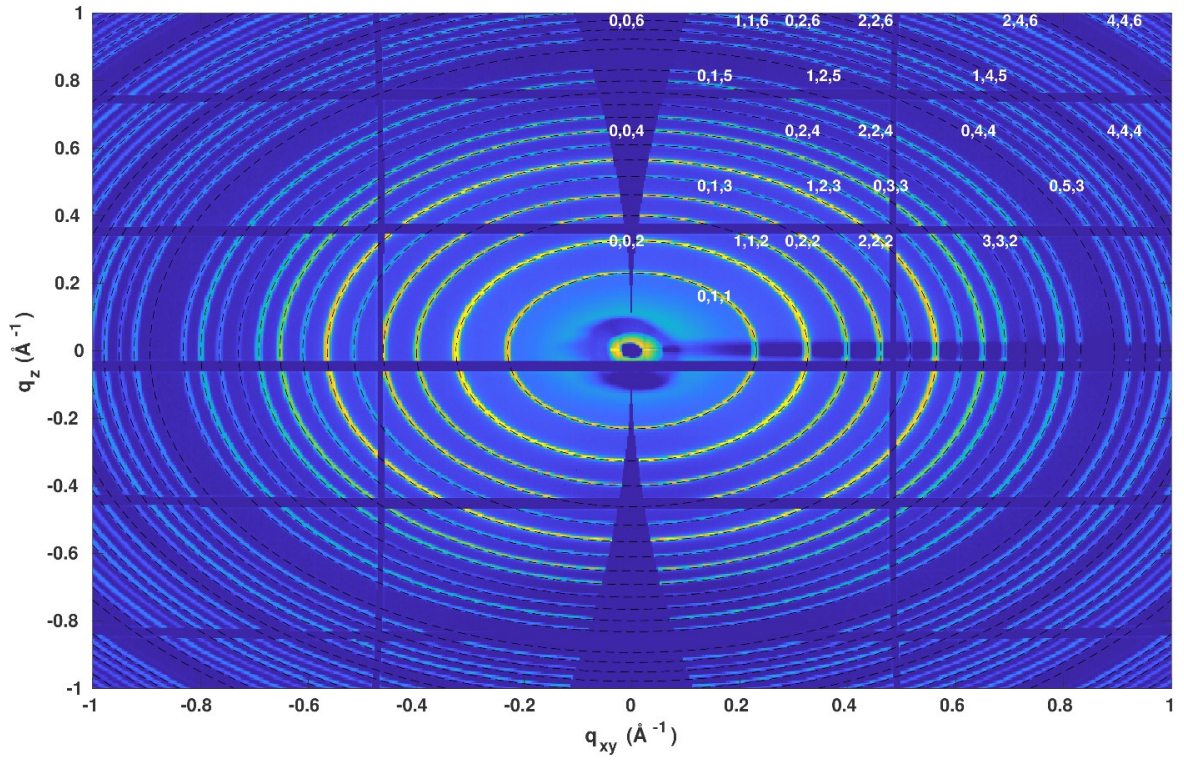

Fig. S3. Synchrotron PXRD patterns of Pt(II)PCN-224. The dashed lines are the peak positions determined by a structure generated by replacing the Ni atoms of Ni(II)PCN-224 from Ref [6] by Pt atoms. The labels in white are the Laue indices.

In the next step also the relative intensities of the peaks are compared between the model structures (Ni(II)PCN-224, Pt(II)PCN-224) and the measured data. For this comparison we integrated the intensity over the entire PXRD pattern (shown in Fig. S2 and S3) and these data are then normalized to the maximum intensity. As a logical next step these data are compared to calculated PXRD patterns of the model structures. These calculations were performed using the Mercury software package.[7–11] The obtained results are shown in Fig. S4 and S5. One can see that for both model systems Ni(II)PCN-224 and Pt(II)PCN-224 the relative intensities of all peaks agree well with the relative intensities determined in the experiment. Two peaks with rather weak experimental intensities (013 and 123) better agree to the Pt(II)PCN-224 data which can be directly explained by the larger atomic number of Pt and the resulting larger scattering factor. These peaks are hardly detectable for the Ni containing system, but can be measured for the Pt system, which is what we see in the experiment. Based on these observations one can conclude that the newly synthesized Pt(II)PCN-224 MOF adopts the structure of Ni(II)PCN-224, with Ni atoms being replaced by Pt atoms. Nevertheless, a refinement of the unit cell parameter (lattice vectors a=b=c) has been performed by using the program PowderCell.[12] The lattice parameter was varied and the resulting PXRD pattern was compared to the experimental one. This refinement procedure resulted in a lattice vector of 38.62 Å. For this lattice parameter we find a good agreement between experiment and model (see Fig. S6). Some structural information for this system is given in Table S1.

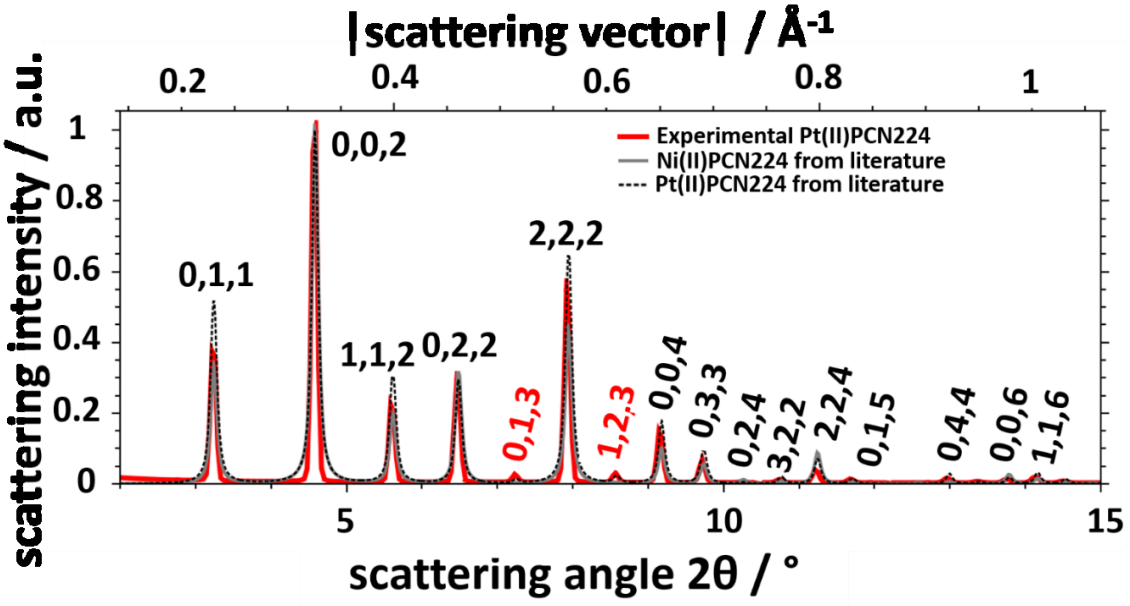

Fig. S4. Normalized PXRD data shown as a line graph. The data was extracted by integrating over the intensity of the experimental PXRD pattern and normalized to the maximum intensity. The data for the model structures was calculated by using the Mercury software package. The scattering angle has been calculated for a wavelength of 1.5406 Å (Cu-Kα_1).

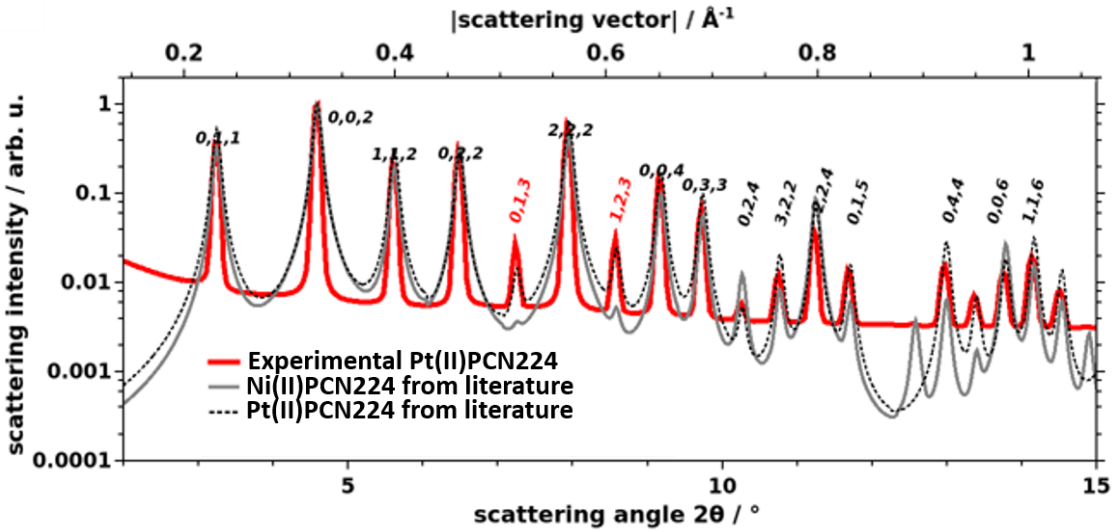

Fig. S5. Normalized PXRD data shown as a line graph with a logarithmic intensity scale. The data for the model structures was calculated by using the Mercury software package.

Table S1. Structure information for Pt(II)PCN-224, based on Ref [6].

space group	Im-3m
refined lattice vector (a=b=c)	38.62 Å
cell angle α=β=γ	90°

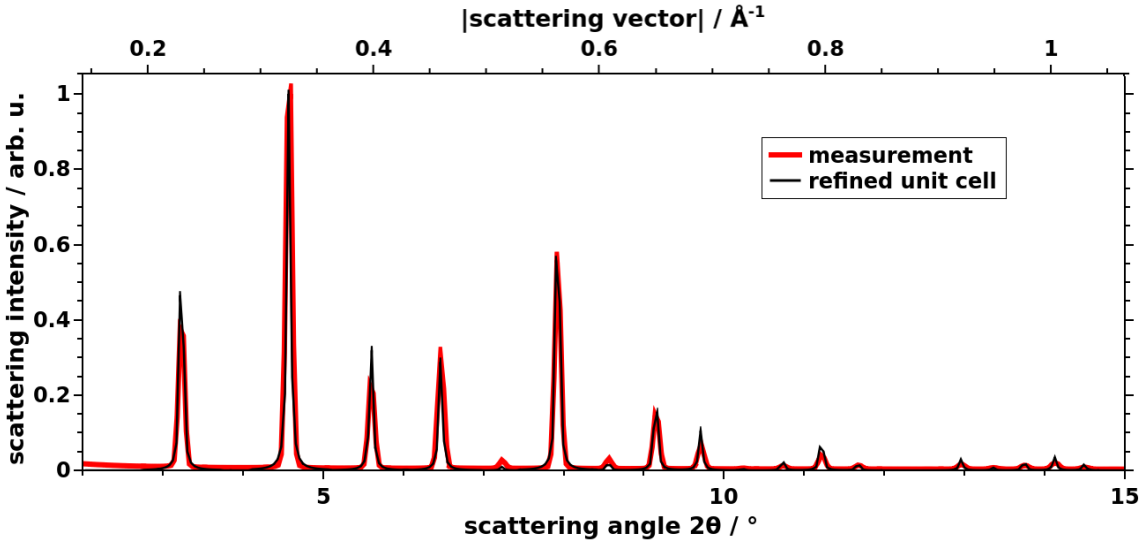

Fig. S6. Comparison of the measured PXRD data to the refined model of Pt(II)PCN-224 with a lattice parameter of 38.62 Å. The scattering angle has been calculated for a wavelength of 1.5406 Å (Cu-Kα_1).

PCN-224:

The results for PCN-224 have been analyzed analogously to the steps described above for Pt(II)PCN-224. The synchrotron PXRD pattern is shown in Fig. S7 and the extracted line graph is presented in Fig. S8.

By comparing peak positions and relative intensities between the measured data and the data calculated for the literature structure one can conclude that the synthesized MOF exhibits the structure reported for PCN-224 in Ref [6]. Despite this good agreement it seems that all the experimental peaks are slightly shifted towards lower angles (see Fig. S8), which would correspond to larger unit cell parameters. As this is true for all observed peaks and as the system has cubic symmetry this could for example be rationalized by different temperatures of the measurement here and in Ref [6]. Isotropic volumetric expansion could lead to such shifts of the peaks. Refining the unit cell parameter based on the measured data by using the program PowderCell[12] and employing the same methodology as described above one can actually find a slightly enlarged lattice parameter of 38.61 Å. Nevertheless, we can safely conclude on the synthesized material exhibiting the literature reported structure,[6] with the refined lattice parameter of 38.61 Å. In Table S2 some structural information can be found for PCN-224.

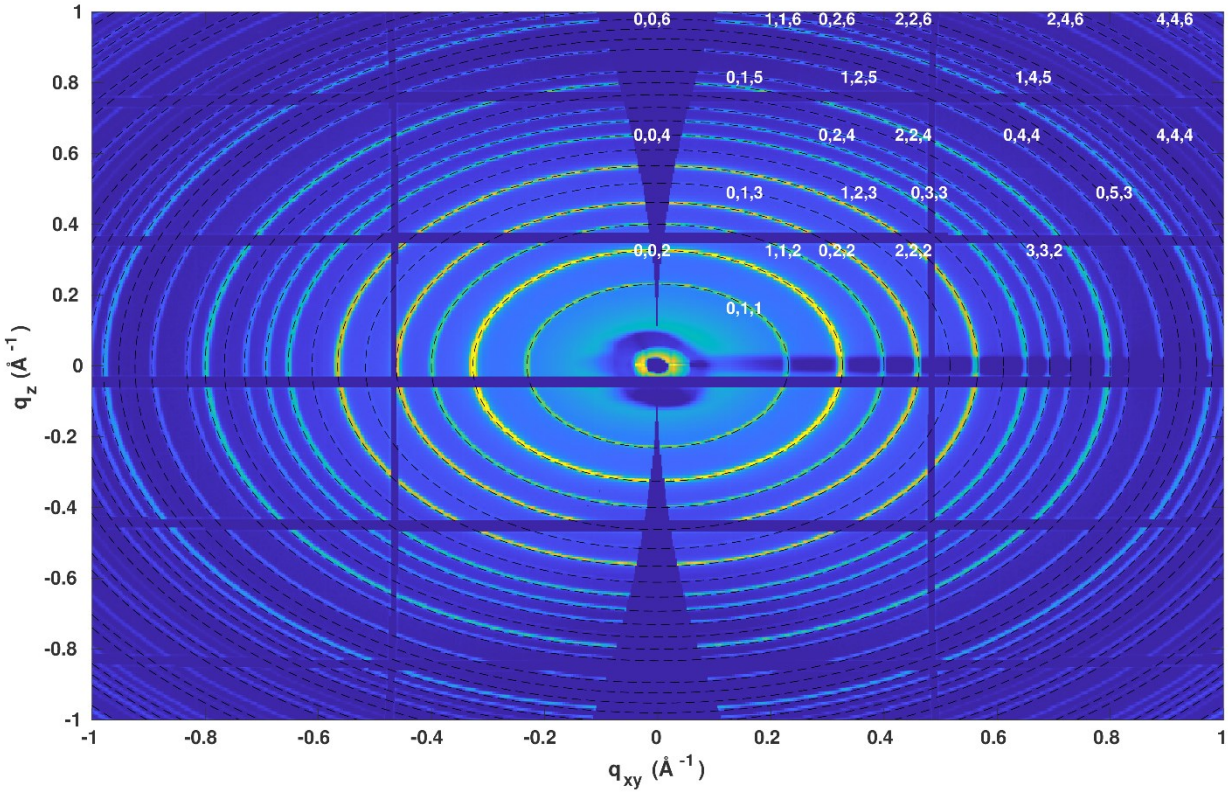

Fig. S7. Synchrotron PXRD patterns of PCN-224. The dashed lines indicate the peak positions of the literature structure of PCN-224.[6] Compared to Pt(II)PCN-224, several peaks are no longer visible (e.g. 013 or 123).

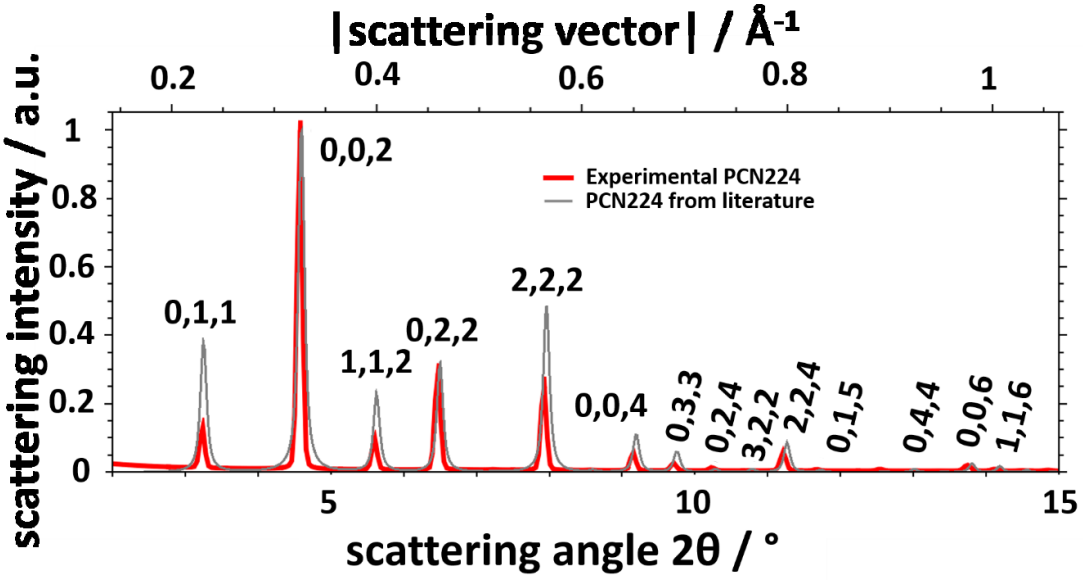

Fig. S8. Normalized PXRD data shown as a line graph. The data was extracted by integrating over the intensity of the experimental PXRD pattern and normalized to the maximum intensity. The data for the model structures was calculated by using the Mercury software package. The scattering angle has been calculated for a wavelength of 1.5406 Å (Cu-Kα_1).

Table S2. Structure information for PCN-224, based on Ref [[6]].

space group	Im-3m
refined lattice vector (a=b=c)	38.61 Å
cell angle α=β=γ	90°

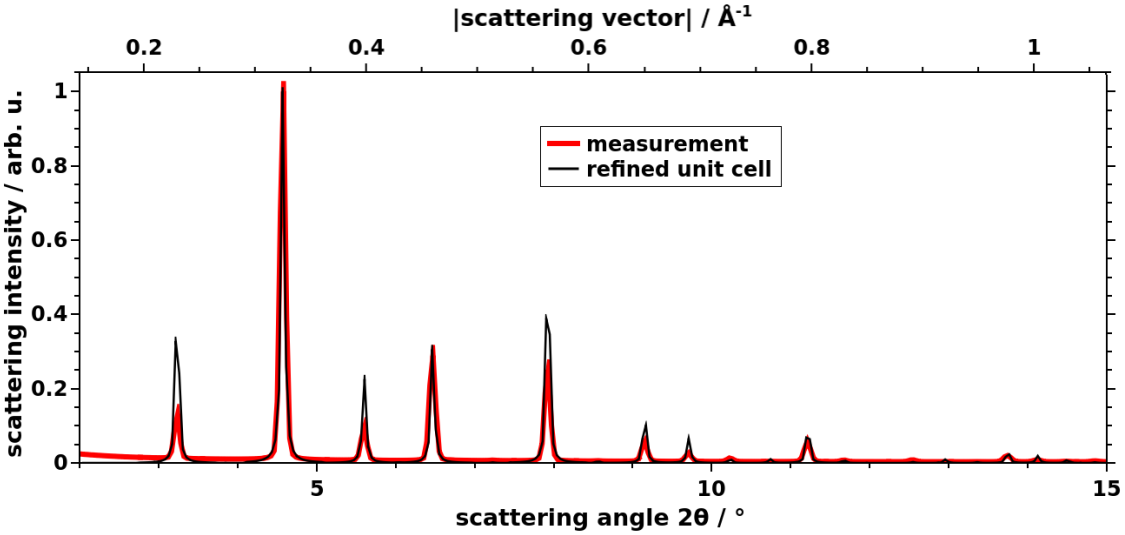

Fig. S9. Comparison of the measured PXRD data to the refined model of PCN-224 with a lattice parameter of 38.61 Å.

PXRD measurement of Pd(II)PCN-224

Powder x-ray diffraction (PXRD) measurements of Pd(II)PCN224 were performed with an PANalytical Empyrean system using a sealed copper tube together with a multilayer mirror for generating a parallelized and monochromatized primary X-ray beam. A wavelength of 1.542 Å was used. The scattered intensity was detected with a PIXcel detector operating in a one-dimensional (1D) mode. The diffraction pattern was converted into a reciprocal space using the equation $q = \frac{4\pi}{\lambda} sin(\Theta)$, with q as the length of the scattering vector, λ as the used wavelength, and 2Θ as the angle between the primary and the scattered X-ray beam. The distance d between the real space planes depends on q as follows: $d = \frac{2\pi}{q}$.The intensity has been normalized to its maximum value within the considered q-range. The results are shown in Fig. S10 and S11.

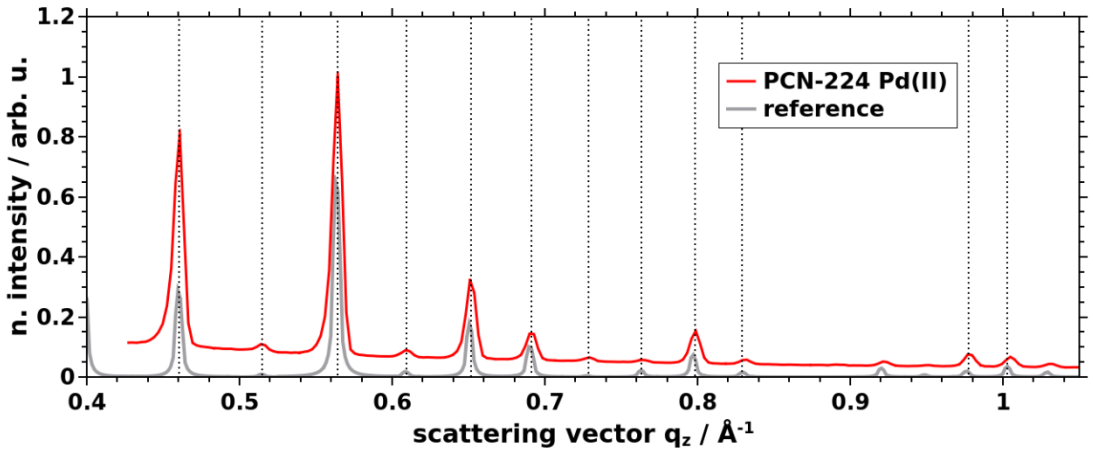

Fig. S10. Powder XRD patterns for the Pd(II) PCN-224 MOF. The grey line indicates the calculated pattern for a reference[6] structure with a lattice constant of 38.62 Å.

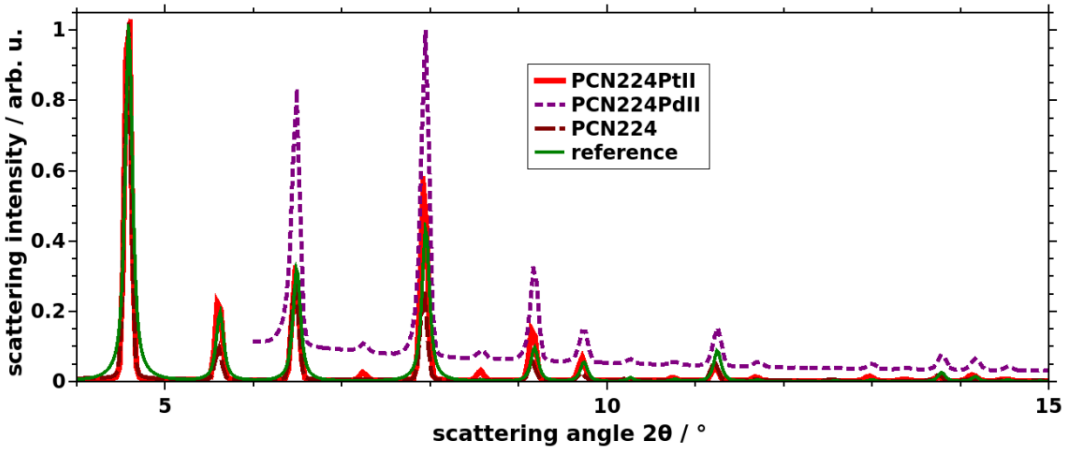

Fig. S11. PXRD of the three MOFs PCN-224, Pt(II)PCN-224 and Pd(II)PCN-224 together with a reference in one plot.

N_2 adsorption isotherms

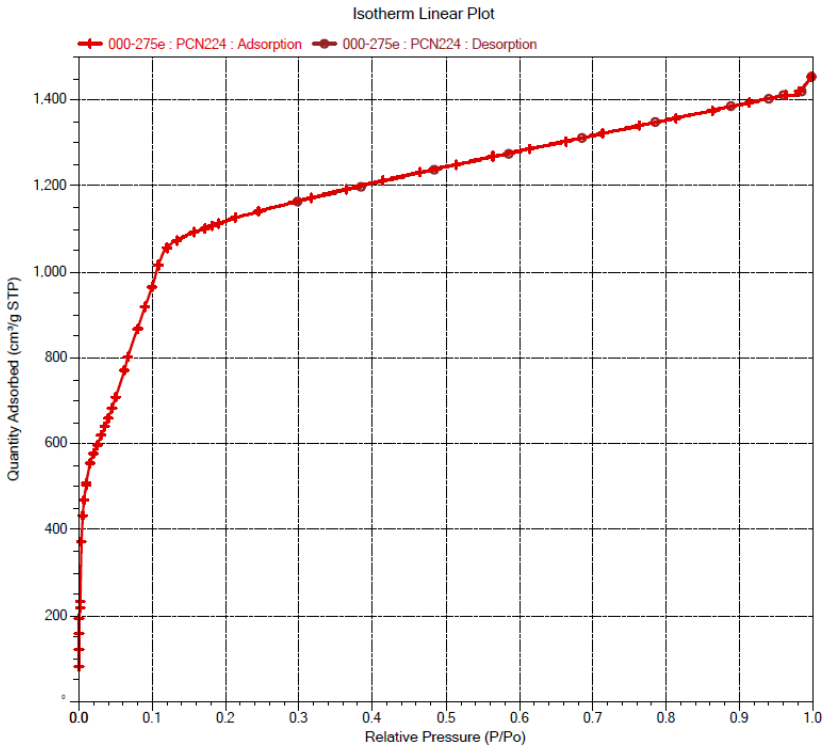

Fig. S12. N_2 adsorption isotherm of PCN-224.

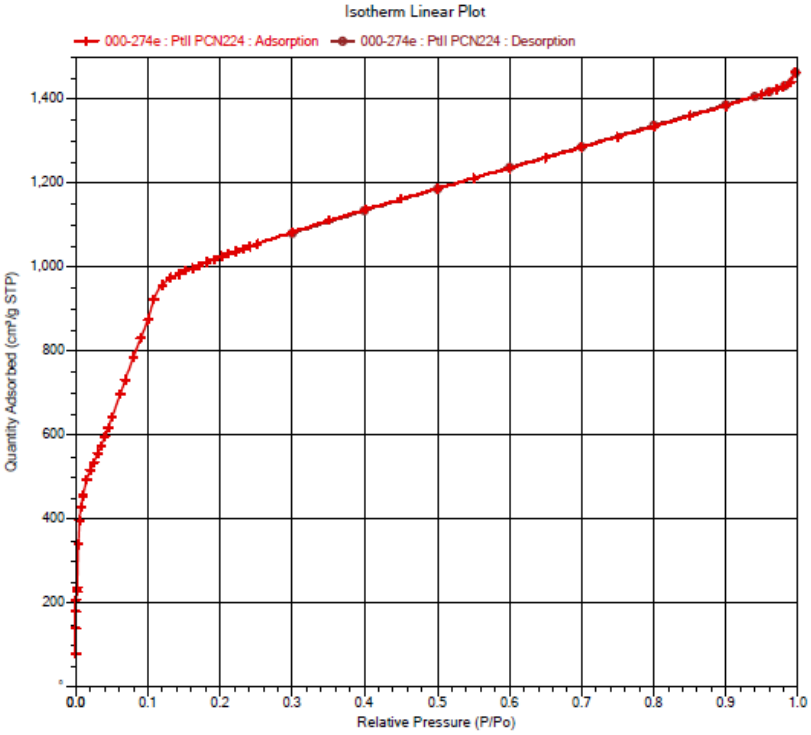

Fig. S13. N_2 adsorption isotherm of Pt(II)PCN-224.

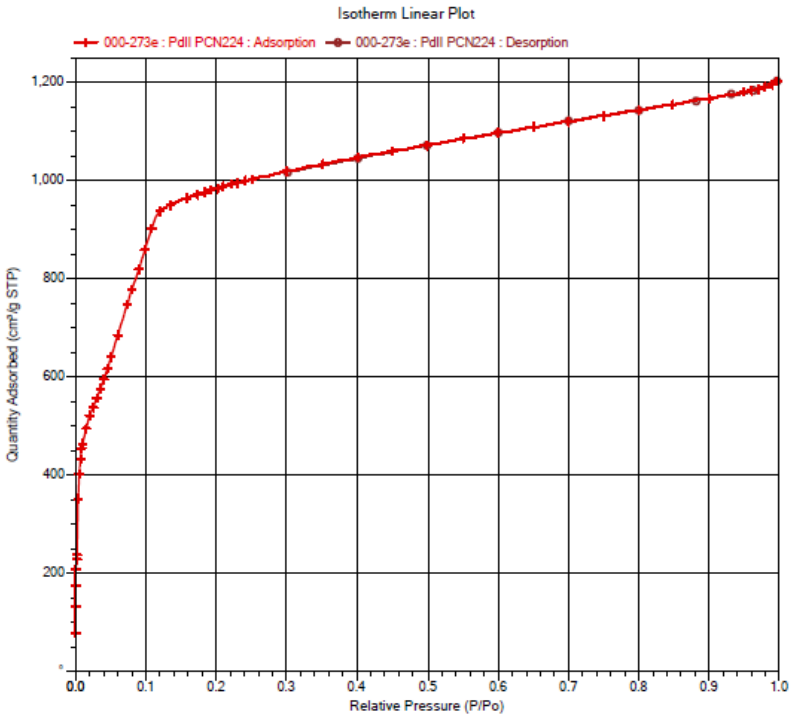

Fig. S14. N_2 adsorption isotherm of Pd(II)PCN-224.

SEM images of PCN-224 free powder

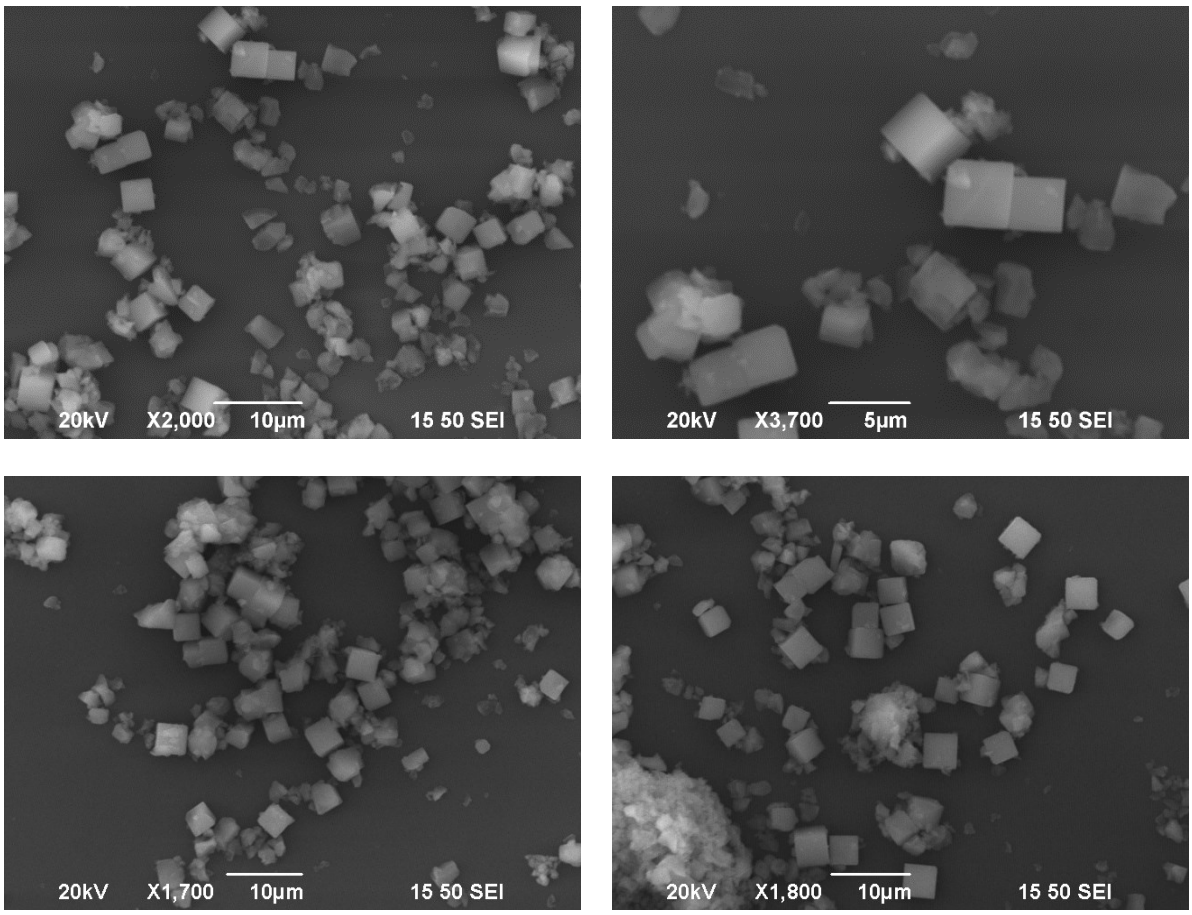

Fig. S15. SEM images of the PCN-224 samples.

SEM images of Pt(II)PCN-224 free powder

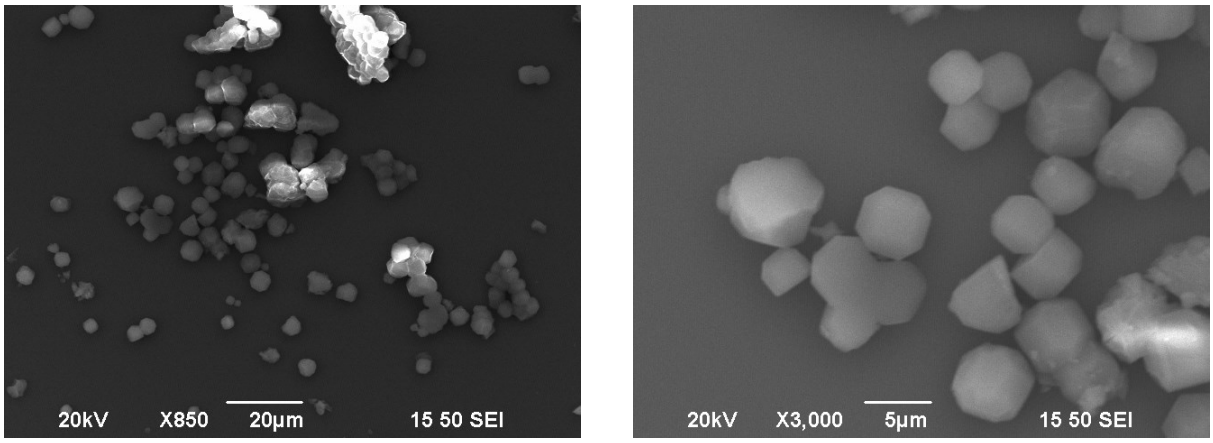

Fig. S16. SEM images of free Pt(II)PCN-224 powder.

SEM images of Pd(II)PCN-224 free powder

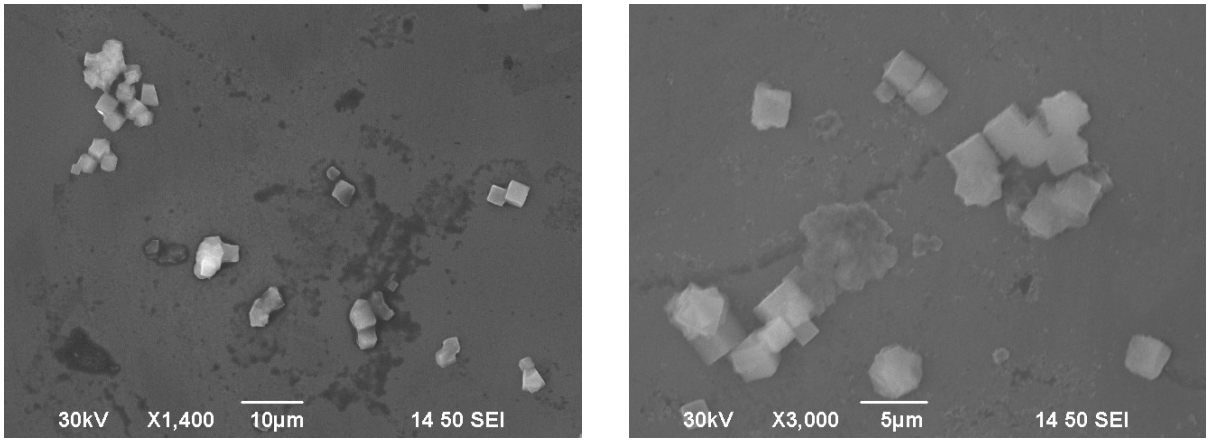

Fig. S17. SEM images of free Pd(II)PCN-224 powder.

SEM images of PCN-224 immobilized on various substrates

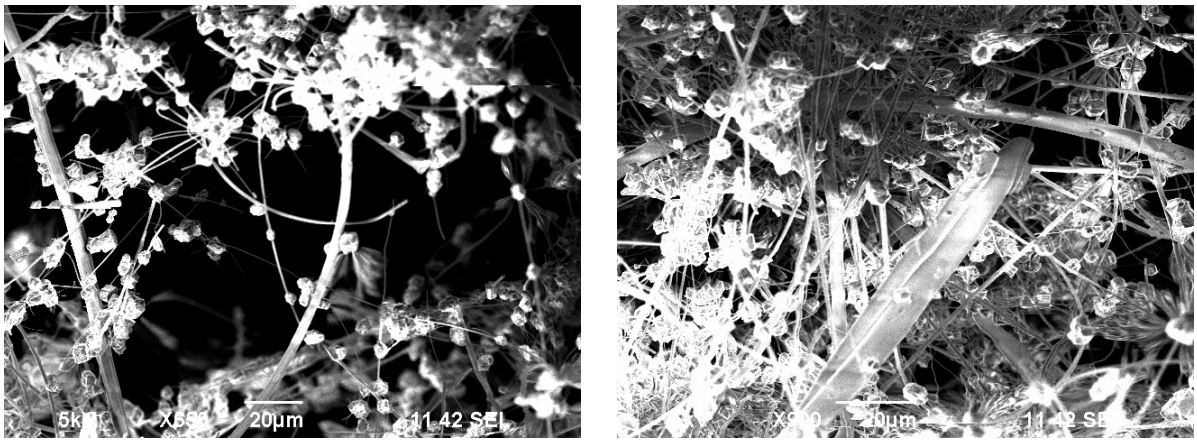

Fig. S18. SEM images of PCN-224 immobilized on glass fiber filter.

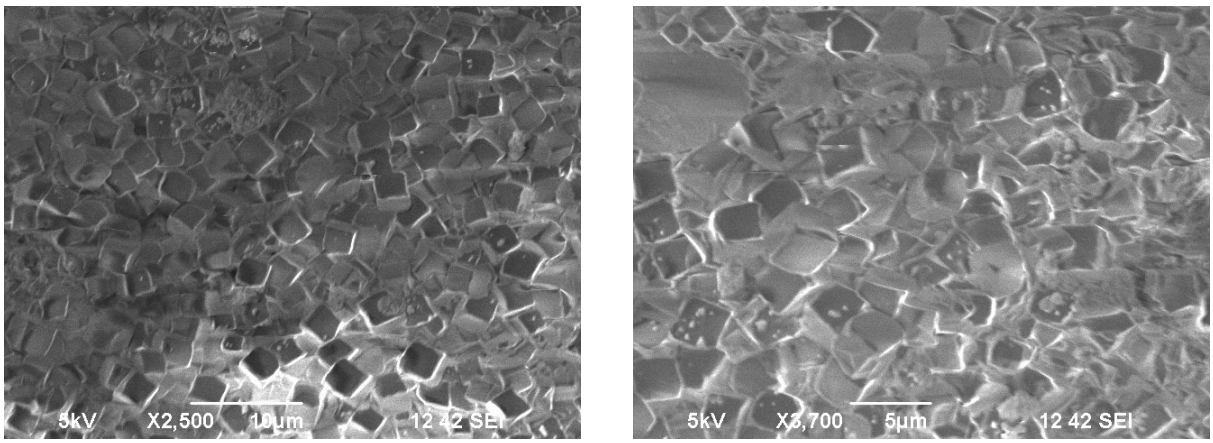

Fig. S19. SEM images of PCN-224 immobilized on poly(amide) filter.

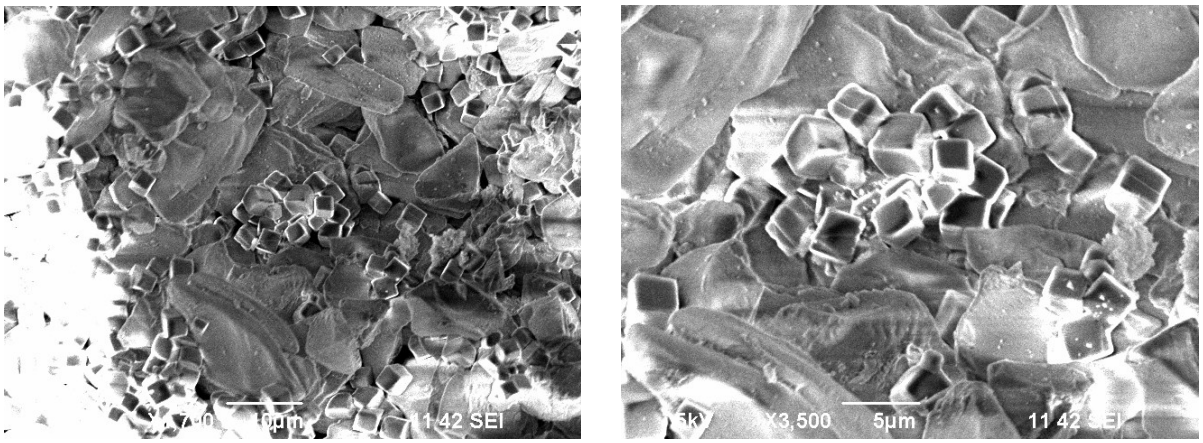

Fig. S20. SEM images of PCN-224 immobilized on aluminum supported silica gel surface (TLC).

Electrospinning of PAN micro/nanofibers

A 10% w/w solution of PAN in DMF was electrospun using a spinneret with a diameter of 0.8 mm. The humidity level was kept at 35% relative humidity throughout the electrospinning procedure and as a collector an aluminum foil covered square copper plate with an area of 16 cm^2 was used. Electrospinning was done using 25 kV DC voltage for 15 minutes. The non-woven fibrous material was collected as a white, stable fiber matt. The PAN fiber matt was easily removed from the substrate with a pair of tweezers.

The PAN micro/nanofibers were then cross-linked by heating them with a controlled temperature increase of 2 °C/min from room temperature to 280 °C. The fibers were kept at 280 °C for 2 h. After cross-linking, the PAN nanofibers were slightly darker and completely insoluble in DMF.

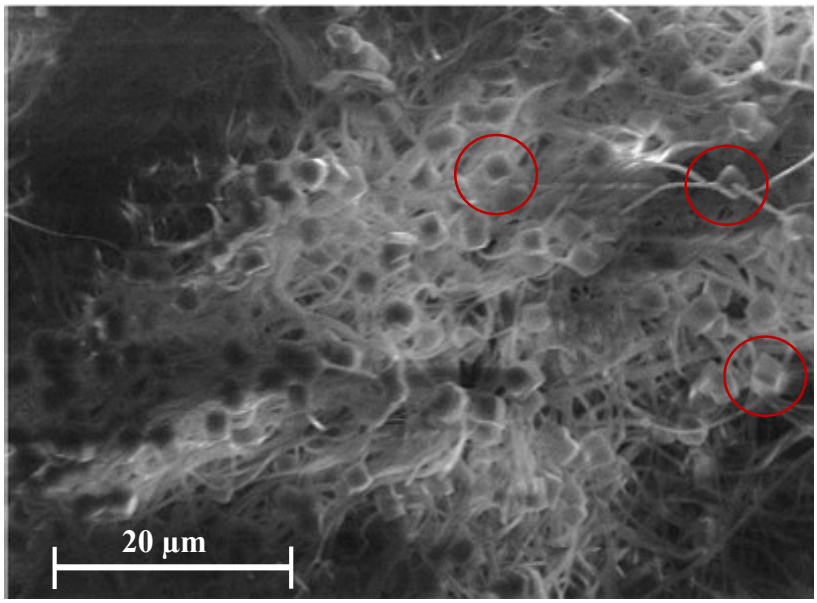

Fig. S21. PCN-224 grown on electrospun PAN nanofibers. Three individual crystals have been marked (red circle).

SEM images of PCN-224 immobilized on PAN as shown on Fig**.** S21 are challenging to acquire because the fiber mats are freely flowing in the SEM chamber. Nevertheless, in the SEM image, the cubical crystals of PCN-224 which grew around individual fibers can be observed.

PXRD of PCN-224 on grown on PAN fibers were compared to two samples PCN-224 to confirm the crystal structure of PCN-224 grown on the fibers (Fig. S22).

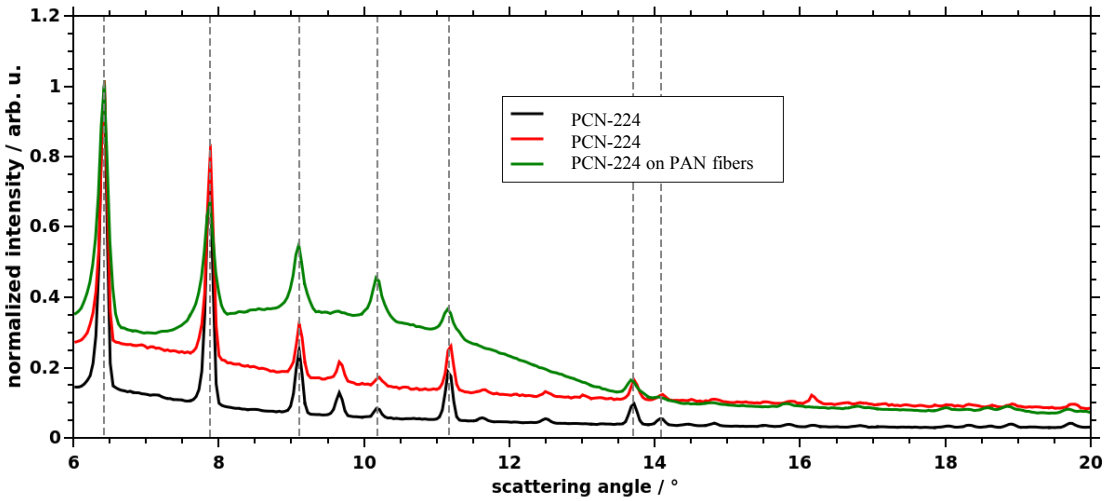

Fig. S22. PXRD Analysis of PCN-224 on PAN fibers compared to two samples of free PCN-224 crystals.

Guidelines for ultratrace oxygen setup:

- Only new 1/8''stainless- steel capillaries from Swagelok (https://www.swagelok.com) were used for the calibration setup. All connections between calibration gas bottles and the measurement chamber were done with new 1/8'' Swagelok connectors which were cleaned, degreased and dried before use.

- The high purity N_2 7.0 (≥99.99999 % purity) was connected as recommended by the supplier with a W 24,32 x 1/14 valve according to DIN 477 Nr. 10.

- According to the specification of the high purity N_2 7.0(≥99.99999 % purity) from Linde (www.linde.com), residual oxygen of 30 ppb or less can be expected. This level of residual oxygen is within the purity obtained by purifying N_2 6.0 with commercially available gas filters for O_2 removal and can therefore considered to be sufficient for ultra-trace oxygen measurements.

- To ensure high precision of gas mixing, mass flow controllers (Voegtlin, red-y s GSC-A4 series, with highest accuracy (+-0.3 % of full scale and +-0.5 % of reading according to specification) were used.

- As a measurement chamber, a 10 mL Schlenk flask was equipped with a steel capillary. The sample to be measured was placed in a glass vial in the Schlenk tube and the sample was excited via optical fibers through the bottom wall of the Schlenk tube.

- The Schlenk tube with the sample was evacuated with a rotary vane pump prior to calibrations to a pressure below 1 mbar and purged with nitrogen prior to measurements.

- To ensure a tight connection between the calibration gas delivery supply and the Schlenk tube, a stainless steel capillary was used to feed the calibration gas directly to the Schlenk tube. The capillary was glued into the Schlenk flask. Moreover, the steel capillary was placed in close proximity to the sample in the Schlenk tube.

- Prior to recording calibration data, the whole piping, including two pressure reduction valves, the mass flow controllers and the capillaries, was purged with descending mixtures of

calibration gas (20ppm O_2 in N_2) and pure N_2 from 20 ppm down to N_2 to ensure oxygen-free conditions at the beginning of the calibration.

- Calibration required an equilibration phase between 1 and 3 calibration cycles to ensure stable calibration.

Setup for temperature controlled calibrations

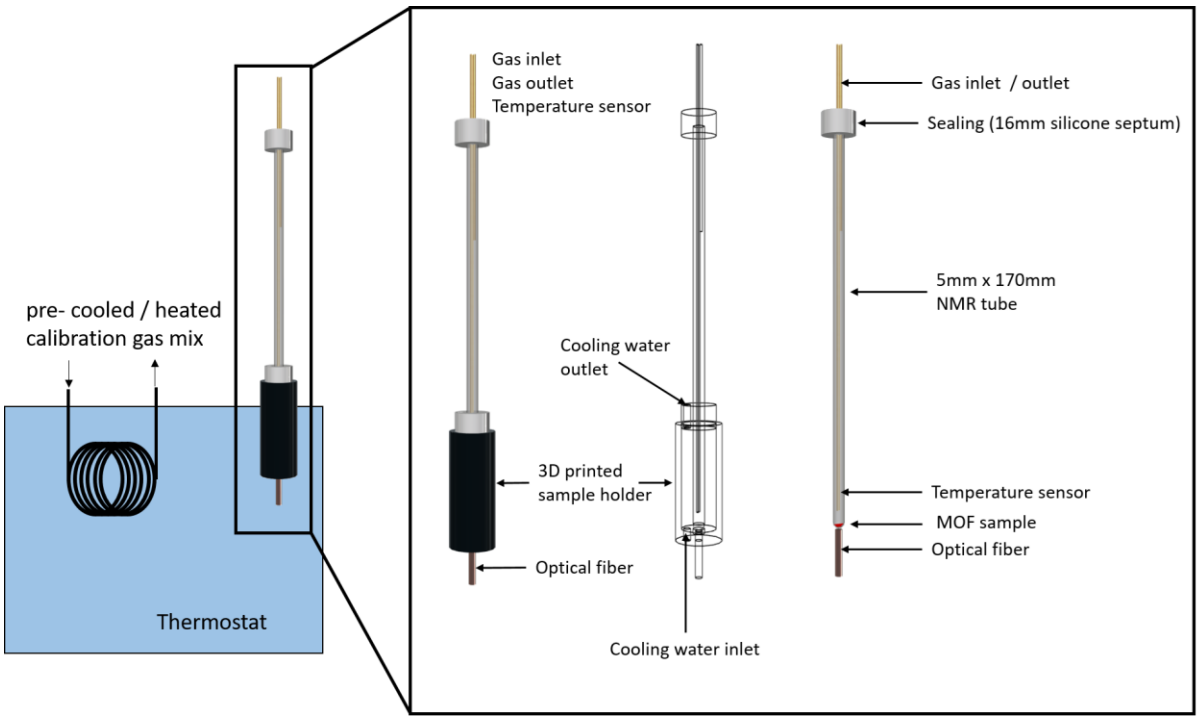

Fig. S23. Sketch of the custom-made setup for calibration under temperature-controlled atmosphere and photobleaching experiments.

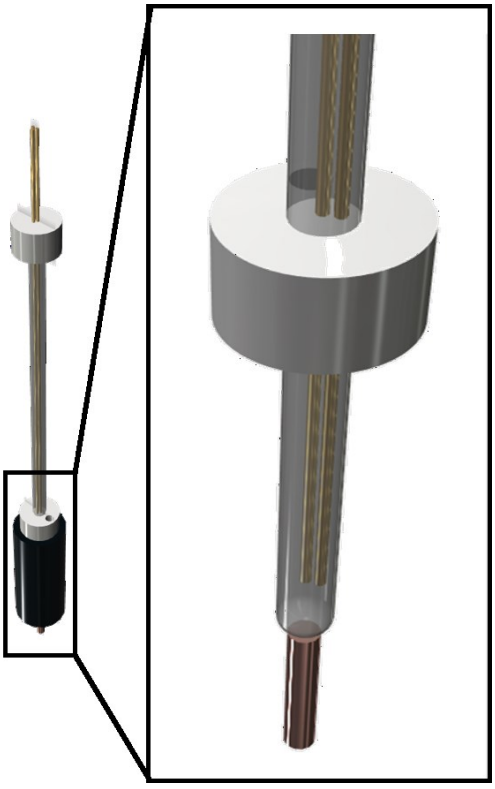

Fig. S24. 3D View of the sample chamber (NMR tube) and optical fiber arrangement.

Temperature dependency of the luminescence quenching of PCN-224 and Pt(II)CPN-224 by oxygen

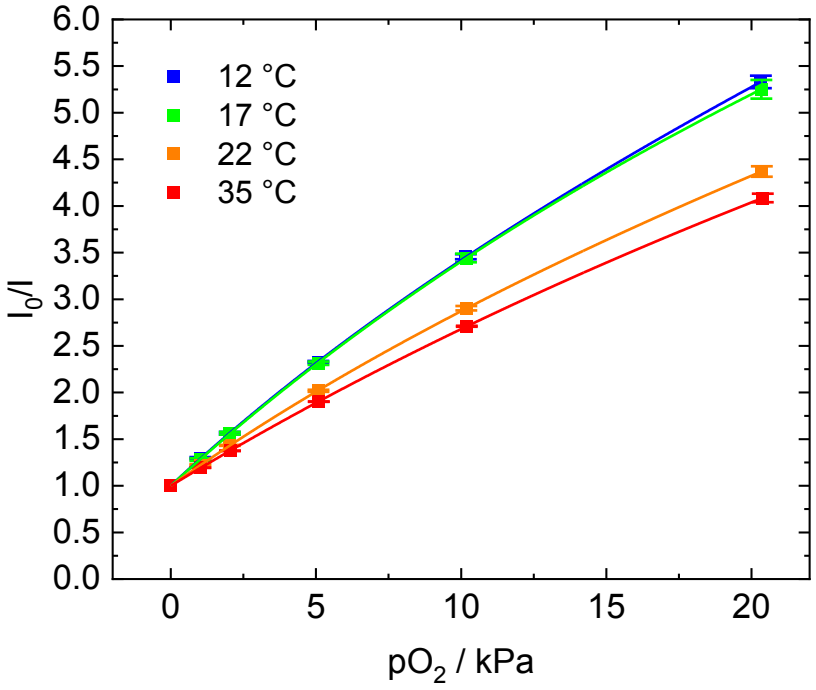

Fig. S25. Temperature influence on fluorescence quenching of PCN-224 by oxygen

Table S3. Fit parameters ("two site model" Fit (Eq. 2)) for the Stern-Volmer plots of PCN-224 obtained at different temperatures.

MOF	Temperature / °C	T0 / ns	KSV_1 / kPa^{-1}	KSV_2 / kPa^{-1}	f
PCN-224	12	6.2	0.320± 0.026	0.0156± 0.022	0.91 ± 0.051
	17	5.8	0.308± 0.008	0.006± 0.005	0.93± 0.012
	22	6.2	0.243± 0.021	0.084±0.014	0.91± 0.05
	35	5.6	0.205± 0.002	0.074± 0.008	0.92± 0.01

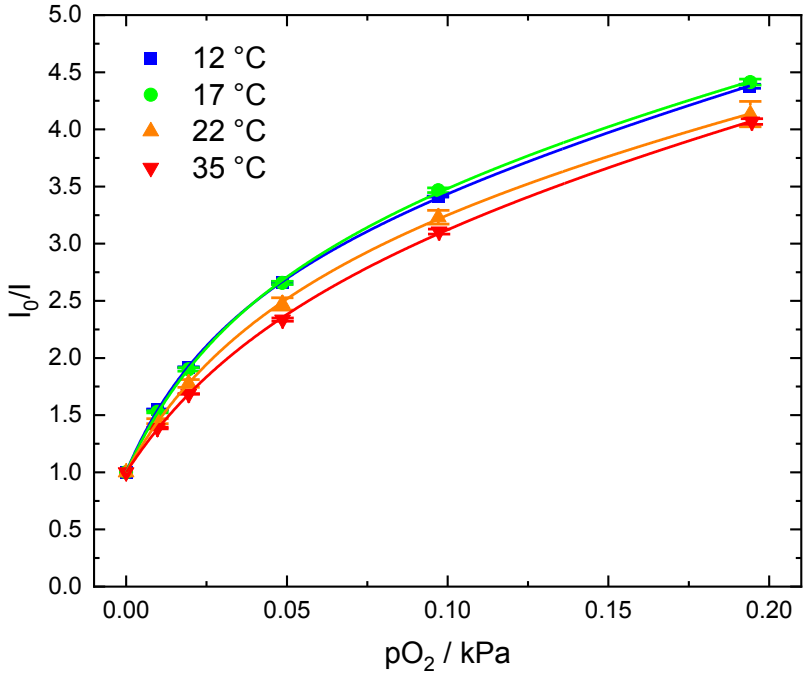

Fig. S26. Temperature influence on luminescence quenching of PCN-224 by oxygen

Table S4. Fit parameters ("two site model" Fit (Eq. 2)) for the Stern-Volmer plots of Pt(II)PCN-224 obtained at different temperatures.

MOF	Temperature / °C	T0 / µs	KSV_1 / kPa^{-1}	KSV_2 / kPa^{-1}	f
Pt(II)PCN-224	12	19.5	89.5 ± 1.94	1.9 ± 0.16	0.75 ± 0.005
	17	19	79.3 ± 4.54	1.41 ± 0.277	0.771 ± 0.012
	22	19.9	66.2 ± 5.07	1.3 ± 0.29	0.76 ± 0.009
	35	19.4	55.4 ± 1.29	1.4 ± 0.20	0.77 ± 0.009

Immobilization of TMCPP in poly(1-trimethylsilyl-1-propyne) (PTMSP) and its sensing properties of the material

A stock solution of PTMSP with a concentration of 10 mg mL^{-1} in toluene was prepared. It was used to prepare the polymer "cocktail" containing 0.5% w/w of TMCPP in respect to the polymer which was knife-coated (25 µm-thick wet layer) on a clean PET support.

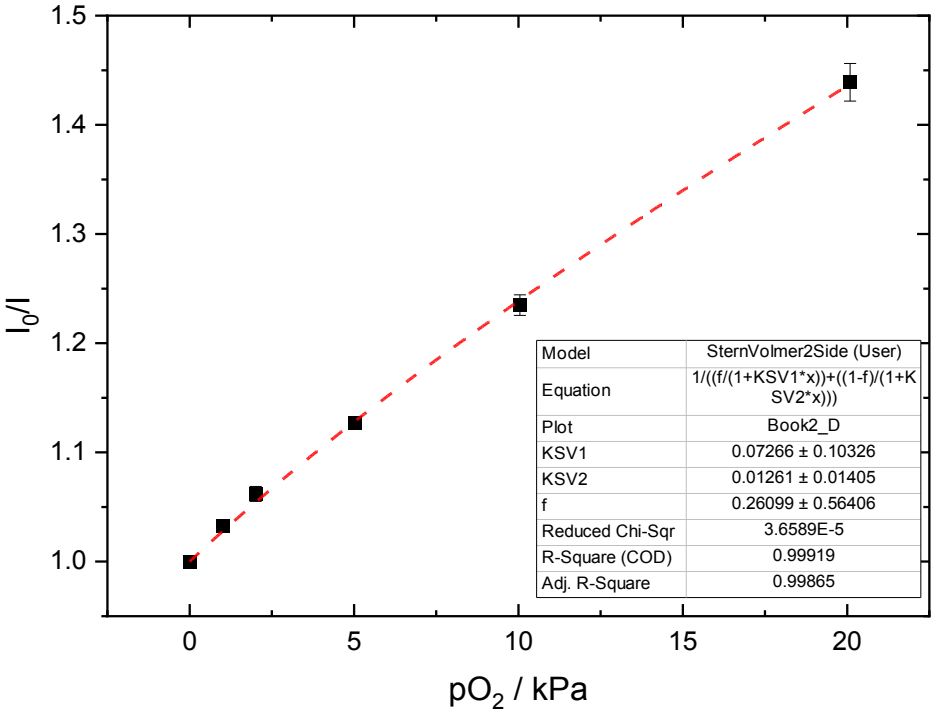

Fig. S27. Stern-Volmer plots of TMCPP immobilized in PTMSP. Fit parameters K_{SV1}, K_{SV2} and *f* can be found in the inlet.

Immobilization of TCPP on aluminum supported TLC silica gel and the sensing properties of the material

10 mg silica gel was stirred with 0.5 mg TCPP in 5mL THF for 20 minutes. Afterwards the silica gel was filtered and washed 3x with 5 mL THF and 3x with 5 mL acetone until no TCPP was found in the filtrate. The slightly colored silica gel was dried at 70 °C under reduced pressure overnight. Calibrations were recorded as described.

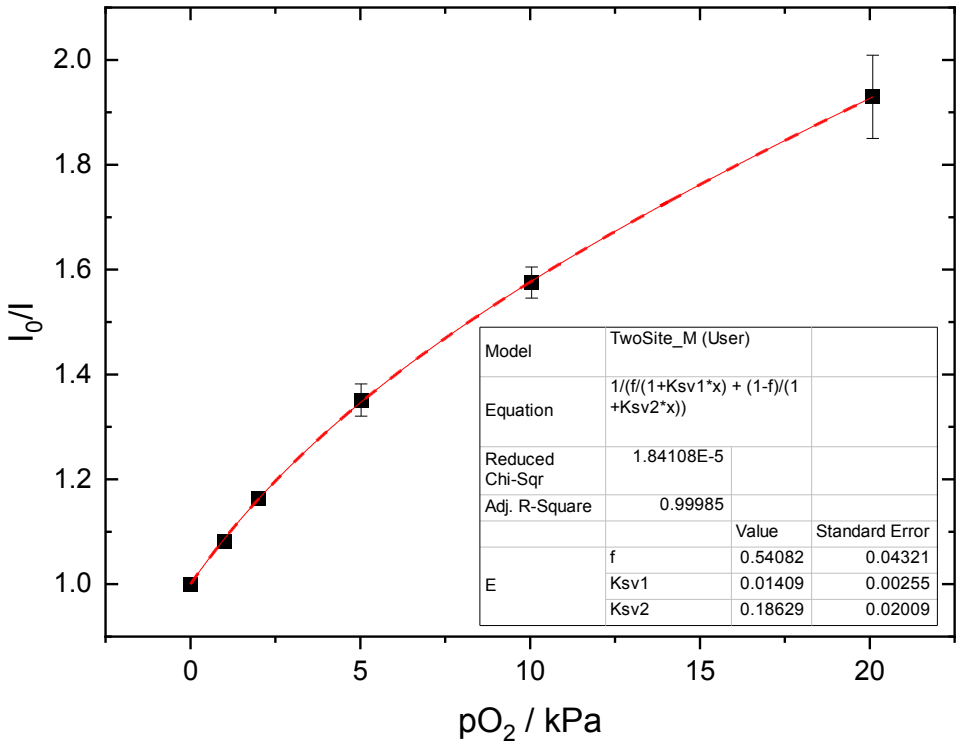

Fig. S28. Stern-Volmer plots of TCPP immobilized on silica gel. Fit parameters K_{SV1}, K_{SV2} and *f* can be found in the inlet.

3D printed equipment for fiber optics

3D printed setup for recording luminescence spectra directly in a Schlenk flask with fiber optics.

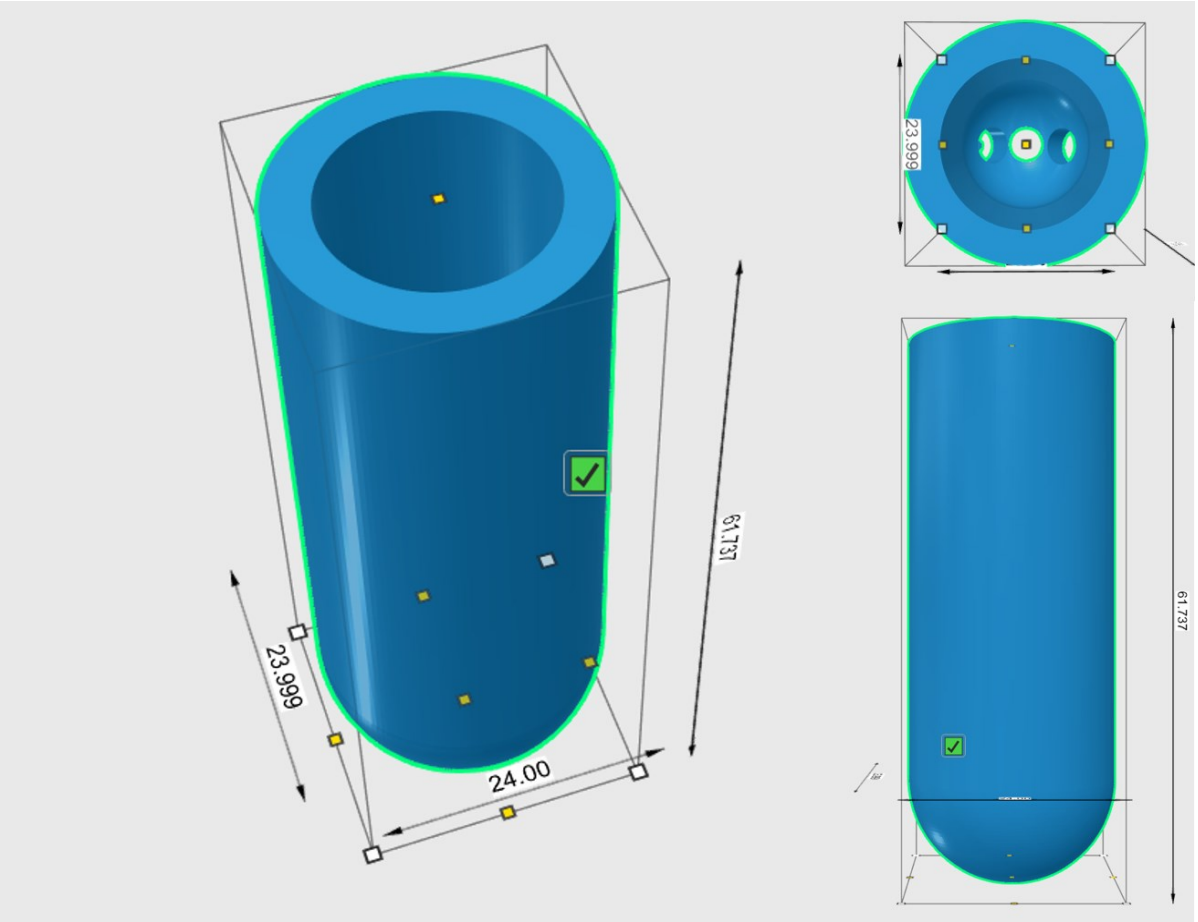

Fig. S29. Design of the 3D printed sample holder for fiber optics and a Schlenk flask.

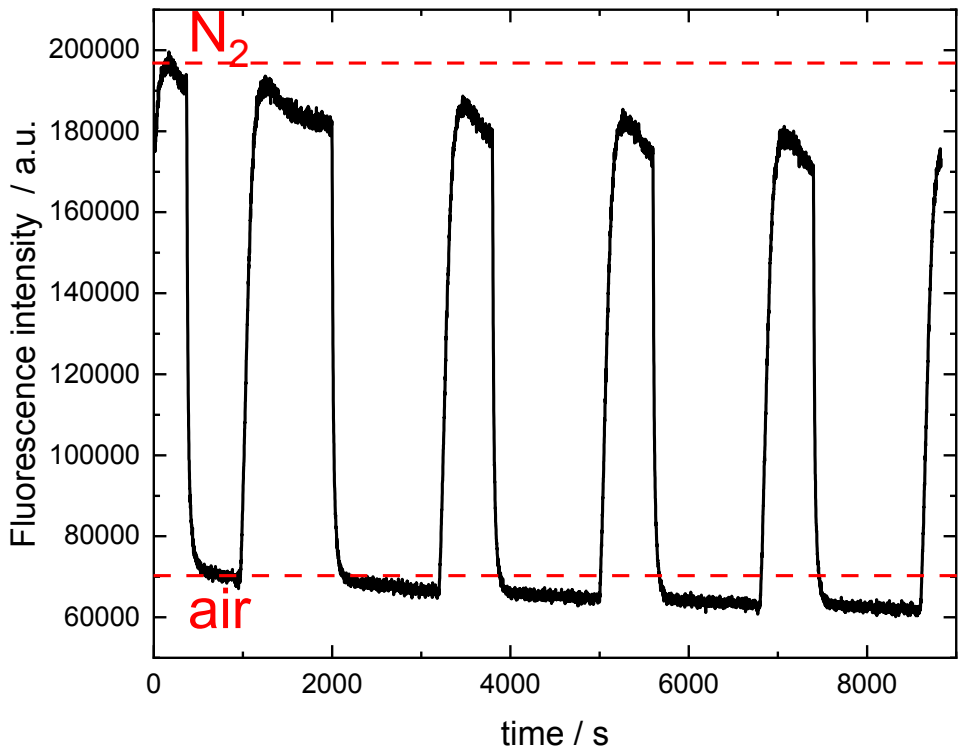

Fig. S30. Photodegradation of PCN-224 under continuous irradiation with a xenon lamp (λ_{exc} = 420 nm, excitation and emission slit: 12 nm).

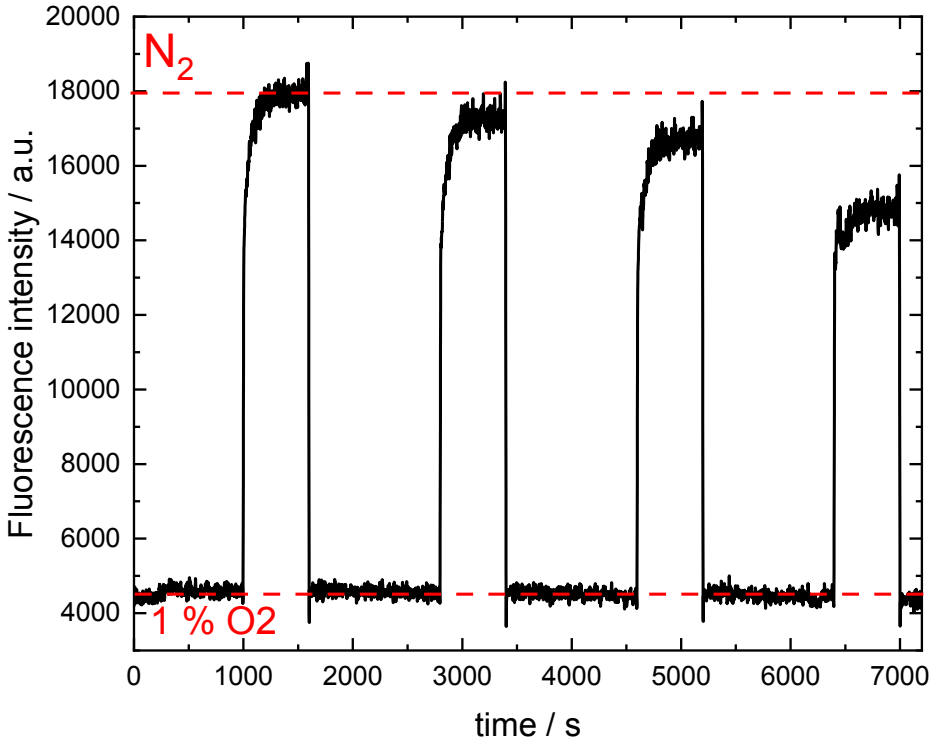

Fig. S31. Photodegradation of Pt(II)PCN-224 under continuous irradiation with a xenon lamp (λ_{exc} = 400 nm, excitation and emission slit: 12 nm).

Table S5. Fit parameters ("two site model" Fit (Eq. 2)) for the Stern-Volmer plots obtained for different samples of PCN-224-based MOFs.

Sensor material	**Measurement mode**	**τ_0**	**K_{SV1} / kPa^{-1}**	**K_{SV2} / kPa^{-1}**	**f**
PCN-224 powder	intensity		0.25±0.01	0.02± 0.02	0.94±0.02
PCN-224 powder	decay time	6.7 ns	0.30±0.09	0	0.84±0.007
PCN-224 @ PAN nanofiber	intensity		0.19±0.002	0	0.97±0.003
PCN-224 @ silica-gel surface	intensity		0.29±0.025	0.01±0.01	0.68±0.03
PCN-224 @ glass fiber	intensity		0.15±0.030	0.01±0.01	0.72±0.10
Pt(II)PCN-224 powder	intensity		73±6	0	0.88±0.01
Pt(II)PCN-224 powder	decay time	18.7 µs	74±5	0.2±0.35	0.88±0.01
Pd(II)PCN-224 powder	intensity		2610±1200	400±200	0.53±0.25
Pd(II)PCN-224 powder	decay time	390 µs	4700±2900	300± 600	0.69±0.32

REFERENCES

1 T. Sakuma, H. Sakai, Y. Araki, T. Wada and T. Hasobe, *Phys. Chem. Chem. Phys.*, 2016, **18**, 5453–5463.
2 S.-Y. Li, B.-R. Xie, H. Cheng, C.-X. Li, M.-K. Zhang, W.-X. Qiu, W.-L. Liu, X.-S. Wang and X.-Z. Zhang, *Biomaterials*, 2018, **151**, 1–12.
3 O. K. Farha, A. M. Shultz, A. A. Sarjeant, S. T. Nguyen and J. T. Hupp, *J. Am. Chem. Soc.*, 2011, **133**, 5652–5655.
4 M. Langsam, M. Anand and E. J. Karwacki, *Gas Separation & Purification*, 1988, **2**, 162–170.
5 B. Schrode, S. Pachmajer, M. Dohr, C. Röthel, J. Domke, T. Fritz, R. Resel and O. Werzer, *Journal of Applied Crystallography*, 2019, **52**, 683–689.
6 D. Feng, W. C. Chung, Z. Wei, Z. Y. Gu, H. L. Jiang, Y. P. Chen, D. J. Darensbourg and H. C. Zhou, *Journal of the American Chemical Society*, 2013, **135**, 17105–17110.
7 C. F. Macrae, I. J. Bruno, J. A. Chisholm, P. R. Edgington, P. McCabe, E. Pidcock, L. Rodriguez-Monge, R. Taylor, J. Van De Streek and P. A. Wood, *Journal of Applied Crystallography*, 2008, 41, 466–470.
8 R. Taylor and C. F. Macrae, *Acta Crystallographica Section B: Structural Science*, 2001, **57**, 815–827.
9 I. J. Bruno, J. C. Cole, P. R. Edgington, M. Kessler, C. F. Macrae, P. McCabe, J. Pearson and R. Taylor, *Acta Crystallographica Section B: Structural Science*, 2002, **58**, 389–397.
10 C. F. Macrae, P. R. Edgington, P. McCabe, E. Pidcock, G. P. Shields, R. Taylor, M. Towler and J. Van De Streek, *Journal of Applied Crystallography*, 2006, 39, 453–457.
11 C. F. MacRae, I. Sovago, S. J. Cottrell, P. T. A. Galek, P. McCabe, E. Pidcock, M. Platings, G. P. Shields, J. S. Stevens, M. Towler and P. A. Wood, *Journal of Applied Crystallography*, 2020, **53**, 226–235.
12 W. Kraus and G. Nolze, *Journal of Applied Crystallography*, 1996, **29**, 301–303.